

Pavel Kůs

Convergence and stability of higher-order finite element solution of reaction-diffusion equation with Turing instability

In: Jan Brandts and Sergey Korotov and Michal Křížek and Karel Segeth and Jakub Šístek and Tomáš Vejchodský (eds.): Application of Mathematics 2015, In honor of the birthday anniversaries of Ivo Babuška (90), Milan Práger (85), and Emil Vitásek (85), Proceedings. Prague, November 18-21, 2015. Institute of Mathematics CAS, Prague, 2015. pp. 140–147.

Persistent URL: <http://dml.cz/dmlcz/702972>

Terms of use:

© Institute of Mathematics CAS, 2015

Institute of Mathematics of the Czech Academy of Sciences provides access to digitized documents strictly for personal use. Each copy of any part of this document must contain these *Terms of use*.



This document has been digitized, optimized for electronic delivery and stamped with digital signature within the project *DML-CZ: The Czech Digital Mathematics Library*
<http://dml.cz>

CONVERGENCE AND STABILITY OF HIGHER-ORDER FINITE ELEMENT SOLUTION OF REACTION-DIFFUSION EQUATION WITH TURING INSTABILITY

Pavel Kůs

Institute of Mathematics, Czech Academy of Sciences
Žitná 25, 1115 67 Praha 1, Czech Republic
kus@math.cas.cz

Abstract: In this contribution, higher-order finite element method is used for the solution of reaction-diffusion equation with Turing instability. Some aspects concerning convergence of the method for this particular problem are discussed. Our numerical tests confirm the convergence of the method, but for some very special choices of parameters, this convergence has very uncommon properties.

Keywords: convergence, finite element method, Turing instability, reaction-diffusion

MSC: 65N30, 35K57

1. Introduction

In this contribution we investigate convergence of higher-order finite element method for a reaction-diffusion problem exhibiting the Turing instability. The motivation of this work is to investigate convergence properties. There is not enough theoretical results regarding convergence theory for this particular application, so we try to observe some properties by performing numerical tests. We are interested in steady-state solutions only, which makes numerical experiments rather time demanding, since a lot of time steps have to be done before the steady-state solution is reached. It is known, that different initial conditions might lead to different steady states. Our interest is to investigate how the choice of finite element mesh and polynomial order influences the resulting steady state. In other words, we are interested in stability of the calculation with respect to choice of finite element approximation.

We are aware of the fact, that the selected method is not the most efficient for the given geometry and equation. There are different methods, which are able to exploit the square geometry such as FFT-based approach (used in [6]) or multigrid method, which is used to solve a similar problem in [4]. Our main interest is, however,

in testing the performance of higher-order FEM and we use this problem as a test example with certain unpleasant properties.

2. Turing instability

Reaction-diffusion equations are studied in various contexts. Our motivation is the study of systems exhibiting the Turing instability. In many applications, the equations describe an interaction of activator u and inhibitor v , see [5] for more motivation and explanations and [2] for more analysis and interesting applications. The investigated problem is the following:

$$\begin{aligned}\frac{\partial u}{\partial t} &= D\delta\Delta u + \alpha u + v - r_2 uv - \alpha r_3 uv^2, \\ \frac{\partial v}{\partial t} &= \delta\Delta v + \gamma u + \beta v + r_2 uv + \alpha r_3 uv^2.\end{aligned}\tag{1}$$

We will consider square domain $\Omega = [0, 200]^2$ and homogeneous Neumann boundary conditions for both u and v . As in the work [5], we will use the following coefficients, which are selected in such a way, that the Turing (“diffusion driven”) instability leads to formation of patterns in the steady-state solution:

$$\alpha = \gamma = 0.899, \quad \beta = -0.91, \quad D = 0.45, \quad r_2 = 2, \quad r_3 = 3.5.\tag{2}$$

Parameters are fine-tuned in such a way, that Turing patterns develop, as can be seen in Fig. 1.

We will consider different values of scaling parameter δ , which can be viewed either as a ratio between the strength of diffusion and reaction or as a measure of the domain size. This choice will affect the appearance of the steady-state solution, as can be seen in Fig. 2.



Figure 1: Left: initial condition used for all following calculations. Middle and right: two intermediate time steps for the value $\delta = 24$. The corresponding steady-state solution is in Fig. 2 in the middle.

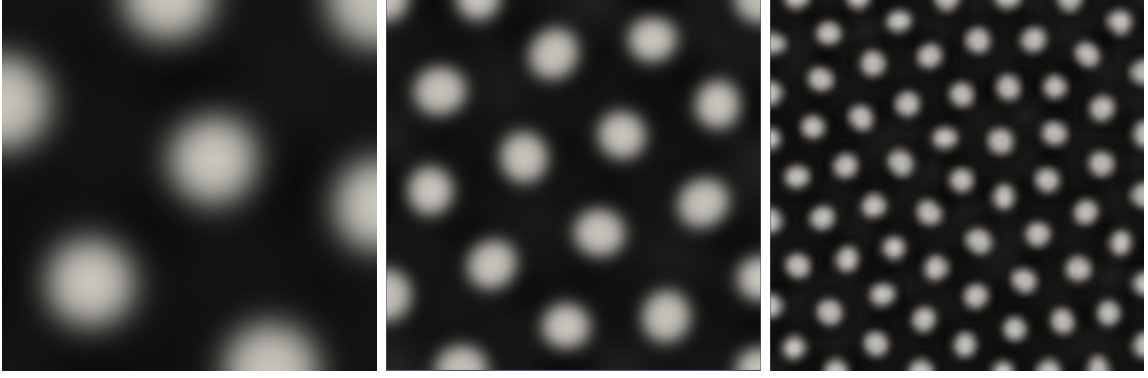


Figure 2: Steady state solutions for the value $\delta = 96, 24$ and 6 , respectively.

3. Discretization

In this contribution, we will not explore more sophisticated time discretization schemes of higher order or adaptive choice of the time step length (as it is done in, e.g., [3]). We will use standard Crank-Nicolson method of second order with time levels t_n and fixed time step $dt = t_{n+1} - t_n$. Moreover, nonlinear terms of (1) will be treated explicitly. After the time semi-discretization, we obtain

$$\begin{aligned} \frac{u^{n+1} - u^n}{dt} &= \frac{1}{2}(D\delta\Delta u^{n+1} + \alpha u^{n+1} + v^{n+1} + D\delta\Delta u^n + \alpha u^n + v^n) \\ &\quad - r_2 u^n v^n - \alpha r_3 u^n (v^n)^2, \\ \frac{v^{n+1} - v^n}{dt} &= \frac{1}{2}(\delta\Delta v^{n+1} + \gamma u^{n+1} + \beta v^{n+1} + \delta\Delta v^n + \gamma u^n + \beta v^n) \\ &\quad + r_2 u^n v^n + \alpha r_3 u^n (v^n)^2, \end{aligned} \quad (3)$$

where u^n and v^n are solutions at time t_n . The space discretization of the resulting system is done in the usual finite element way. In this contribution we use only structured meshes with square elements with the same size and order in one mesh. We use different element sizes for different meshes and polynomial orders 1 to 4.

We are interested only in resulting steady-state solutions. We consider a solution to be steady-state, when the relative norm of difference of solutions in two consecutive time steps is below a prescribed tolerance 10^{-12} . As we have already stated, for a considered setting with fixed parameters, multiple steady state solutions can be found. The trivial solution $u = v = 0$ is always present. Apart from that, several nontrivial solutions can be found, depending on selected initial condition. These solutions might be qualitatively similar (exhibit the same pattern), but, in the sense of a mathematical function, they are completely different. For the considered setting, most initial conditions lead to steady-state solutions containing dots with similar sizes distributed in similar distances. The exact position and even amount of dots may,

however, be completely different (even when symmetries are taken into account), see, e.g., [6]. For the rest of this contribution, we will use the following initial condition:

$$u_I = \left(1 - \frac{|x - 125|}{25}\right) \left(1 - \frac{|y - 125|}{25}\right) \quad \text{for } (x, y) \in [100, 150]^2, \quad (4)$$

$u_I = 0$ otherwise. It is a piece-wise bilinear “hat”, as can be seen in the left panel of Fig. 1. This function is contained in all finite element spaces used in this contribution, so there are no errors caused by inexact projection of the initial condition.

Practical implementation of the problem has been done using the deal.II library (see, e.g., [1]), which simplifies the use of higher-order basis functions. The temporal discretization has been done by hand inside the weak formulation (Rothe’s method). A sparse direct linear solver has been used. Since the nonlinear part is discretized explicitly, calculations in all time steps have the same matrix, which can be factorized at the beginning. Thus, in each time step, only back substitution has to be performed. Even though, the calculations are very time-demanding, since many time steps have to be performed to obtain steady-state solution. We use constant time step $dt = 0.5$ and run the calculation until the relative norm of the difference of two consecutive solutions is below a prescribed tolerance 10^{-12} . The number of iterations depends on mesh, element order and parameter setting, but might exceed 50 000. Higher-order temporal discretization scheme and adaptive choice of time step could improve the situation, but it is not considered in this study. As can be seen from Fig. 3, steady state solutions for given value of δ converge as element size decreases and the number of degrees of freedom increases. This is the case for most (but not all) values of δ , as will be discussed later in the text.

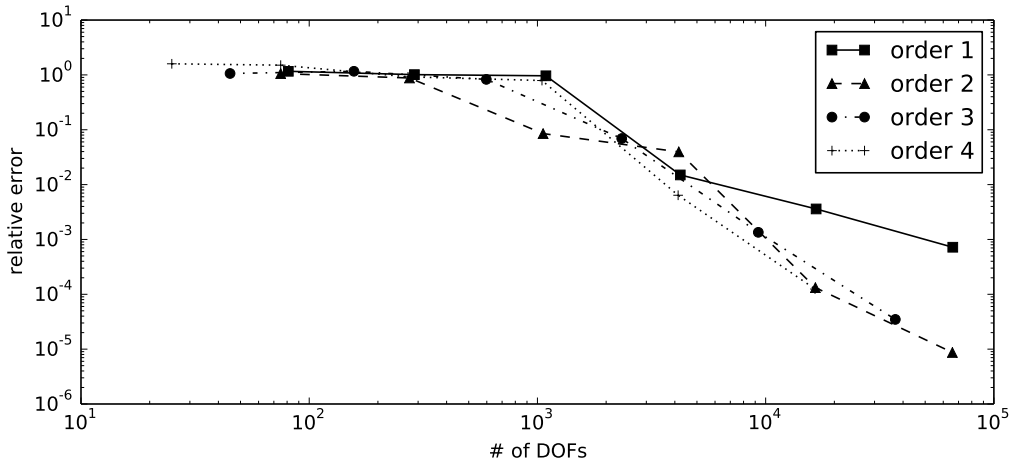


Figure 3: Convergence of FEM solutions for meshes with decreasing element sizes (and thus increasing number of degrees of freedom). The relative norm of difference from the solution on the finest mesh is shown. Results for the value $\delta = 24$.

4. Dependence on parameter δ

Interesting results can be obtained, when the value of the parameter δ is changed with small step. We performed series of calculations with gradually increasing δ , first and last such obtained steady-state solutions are depicted in left and right panel of Fig. 2. Most of the time, continuous dependence of the steady state solution on δ can be observed. Roughly speaking, we can observe that individual dots are getting smaller and their position is changing slowly. At some points, however, there is a bifurcation and a completely different solution is obtained with different number of dots in completely different positions. Many such bifurcations can be seen in Fig. 4, where each peak corresponds to big difference between two consecutive solutions with only slightly different value of δ . A detailed example of one such situation is given in Fig. 5. We remind that the same initial condition (4) is used for all calculations.

Let us now focus more closely on behavior of the solution close to the bifurcation points, where one solution changes to another one. We would like to investigate how this transition occurs, especially with respect to different meshes or polynomial orders. For simplicity, we will (in this contribution) focus only on transition between solutions shown in Fig. 5. For a given mesh, we use interval halving method to estimate the value of the bifurcation point. We do the following series of calculation. At the beginning, we set $\delta_B^1 = 78$, $\delta_B^2 = 79$. Then, at each step, we set $\delta_B = (\delta_B^1 + \delta_B^2)/2$ and find the corresponding steady state solution u_{δ_B} . Then we compare norms of differences of solutions and set $\delta_B^1 := \delta_B$ if $\|u_{\delta_B^1} - u_{\delta_B}\| < \|u_{\delta_B^2} - u_{\delta_B}\|$, or $\delta_B^2 := \delta_B$ otherwise. This process is repeated until $\delta_B^2 - \delta_B^1$ is sufficiently small (10^{-6} in our case). Throughout the whole process, solutions $u_{\delta_B^1}$ and $u_{\delta_B^2}$ are very different, since there is sharp jump between different types of solutions. Originally we thought, that

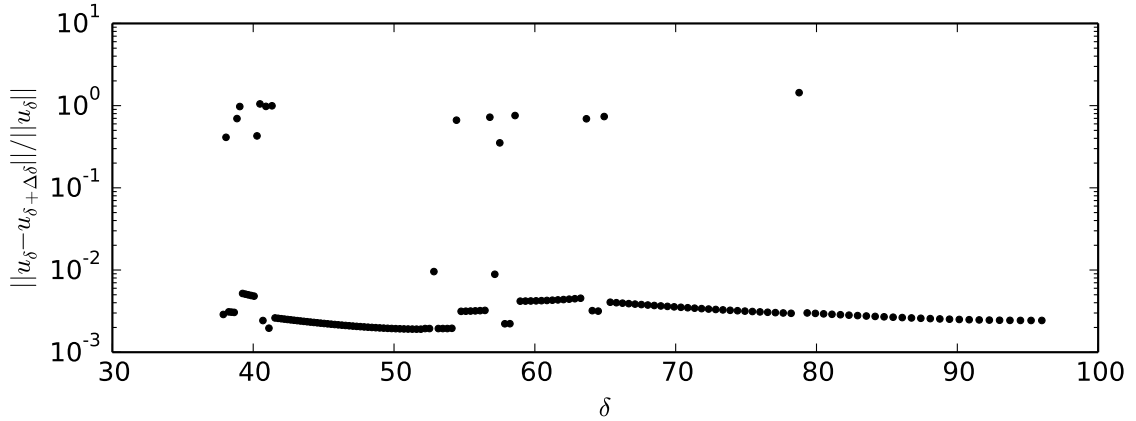


Figure 4: Relative difference of consecutive solutions in a series of calculations with increasing δ . The step $\Delta\delta$ by which δ is increased is approximately $\Delta\delta/\delta = 0.006$. The right-most peak corresponds to the situation from Fig. 5.

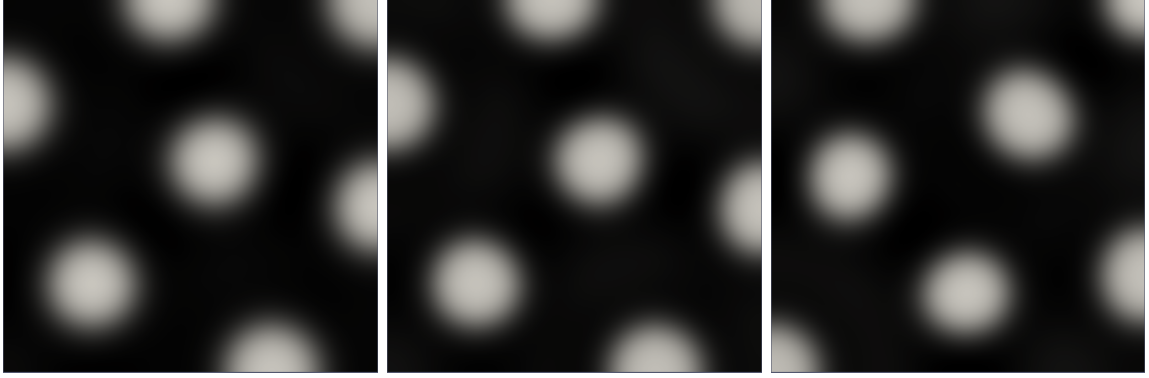


Figure 5: Steady states for value $\delta = 96, 78.76$ and 78.2 , respectively. Even though the difference in parameter is much bigger between first and second value, corresponding solutions are hard to distinguish. The solution for slightly reduced δ is very different (right). This jump corresponds to the right-most peak in Fig. 4.



Figure 6: Steady states obtained on some meshes for $\delta = \delta_B$. These solutions form transition between two types of solutions observed in Fig. 5 and were not observed as peaks in Fig. 4, since the step of change of parameter δ was too large.

this value is the point of transition between solutions from Fig. 5. It turned out, however, that there are (at least) two more solutions obtained numerically (shown in Fig. 6). Values of δ_B obtained by this algorithm for a sequence of consecutively refined meshes can be seen in Fig. 7.

5. Convergence for fixed δ near bifurcation

In the previous section we described dependence of the solution on δ and discussed its behavior close to a bifurcation point. We have seen that this behavior depends on used FEM mesh and polynomial order. This brings us to a natural question, which is the main interest of this contribution. How will this behavior affect convergence of the method close to the bifurcation point δ_B ?

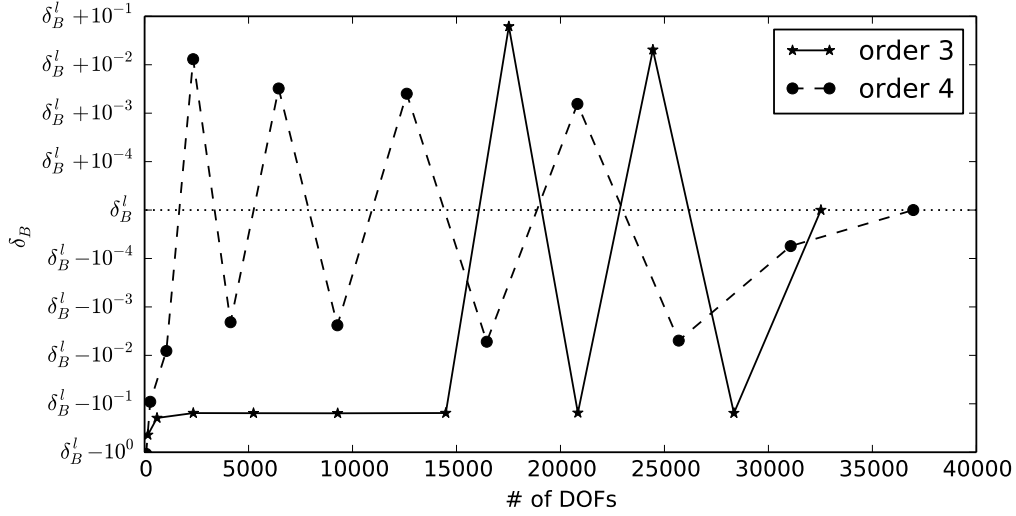


Figure 7: Bifurcation value δ_B for a sequence of consecutively refined meshes. Differences from the “limit” value δ_B^l obtained on the finest mesh are shown. Error in δ_B is less than 10^{-6} , which is sufficiently small compared to differences between values of δ_B for different meshes.

We performed series of calculations with fixed value $\delta = 78.500126$ (which is the “limit” value δ_B^l found by interval halving for finite elements of order 4, see Fig. 7) and with variable number of elements in the mesh. First of all, we found 2 more types of steady state solutions (shown in Fig. 6), distinguished from data presented in Fig. 4. Those new solutions form transition between solutions shown in Fig. 5, which are more “stable” in a sense that they are obtained for δ from a relatively large interval on all used meshes. This is not the case of “transition” solutions from Fig. 6. Another irregularity is the loss of symmetry with respect to line $y = x$, which is present in the initial condition and in all previously observed solutions. These two solutions, however, differ by symmetry with respect to the same axis. The question thus rises whether they really are solutions of the continuous system, or whether they are artificially created by discretization and roundoff errors.

The convergence process can be seen in Table 1. We can observe oscillations rather than smooth convergence. Each of the approximate solutions obtained on meshes with decreasing element size is approaching one of the four “types” of solutions, which are shown in Figs. 5 and 6. We denote them A, B, C and D, respectively. We do not claim that this means that the method does not converge as $h \rightarrow 0$. It may happen, however, that for h in the range given by capabilities of our computer, we are not able to determine, which of the completely different solutions that we are obtaining for different values of h is close to the exact solution for the given δ .

$n :$	16	20	24	28	32	36	40	44	48	52	56	60	64	68	72	76	80
order 3	A	B	A	B	A	B	C	B	C	B	C	B	C	B	D	B	C
order 4	A	C	D	C	C	D	D	D	C	C	D	C	D	D			

Table 1: Types of solutions, obtained by calculation with $\delta = 78.500126$. As A and B we denote solutions from Fig. 5, as C and D solutions from Fig. 6, respectively. Calculations for polynomial orders 3 and 4 are performed on meshes with n elements in each direction, n being the number in the first row. The mesh then consists of n^2 square elements of size $h = 200/n$.

6. Summary

We investigated a particular numerical scheme for the solution of reaction-diffusion problems. We have shown that the method usually converges and that it behaves according to expectations. However, for the parameter value close to a bifurcation point, we observe an oscillating sequence of approximate solutions. Moreover it is possible, that some of the approximate solutions, which are obtained for some meshes, are not approaching any solution of the continuous problem. Even though this behavior can be observed only for carefully selected parameters, we find it interesting, since it opposes the usual idea of convergence of the finite element method.

References

- [1] Bangerth, W., Hartmann, R., and Kanschat, G.: deal.II – a general purpose object oriented finite element library. *ACM Trans. Math. Softw.* **33** (2007), 24/1–24/27.
- [2] Barrio, R. A., Varea, C., Aragn, J. L., and Maini, P. K.: A two-dimensional numerical study of spatial pattern formation in interacting turing systems. *Bulletin of Mathematical Biology* **61** (1999), 483–505.
- [3] Dolejší, V. and Kůs, P.: Adaptive backward difference formula–discontinuous Galerkin finite element method for the solution of conservation laws. *Int. J. Numer. Meth. Engng.* **73** (2008), 1739–1766.
- [4] Landsberg, C. and Voigt, A.: A multigrid finite element method for reaction-diffusion systems on surfaces. *Comput. Visual Sci.* **13** (2010), 177–185.
- [5] Liu, R. T., Liaw, S. S., and Maini, P. K.: Two-stage Turing model for generating pigment patterns on the leopard and the jaguar. *Phys. Rev. E* **74** (2006), 011 914:1–011 914:8.
- [6] Rybář, V. and Vejchodský, T.: Variability of Turing patterns in reaction-diffusion systems. In: H. Bílková, M. Rozložník, and P. Tichý (Eds.), *Proceedings of the SNA'14*, pp. 87–90, 2014.